LIGO-T030186-00-W

Development of a Readout Scheme for High Frequency Gravitational Waves

Jared Markowitz*, Rick Savage, Paul Schwinberg

August 15, 2003

Abstract

The LIGO Hanford Observatory (LHO) interferometers are currently optimized to read data at frequencies between 150Hz and 3000Hz. However, due to the nature of Fabry-Perot Cavities, the sensitivity of the interferometer to length displacement peaks at multiples of the cavity free spectral range (FSR). This increased sensitivity suggests a search for gravitational waves around 37.5 kHz, the FSR of the LHO 4 km interferometer. In this project, a readout channel for gravitational waves at 37.5 kHz in a 900 Hz bandwidth was developed by down-converting the signal to match the existing LIGO data acquisition system. The calibration, sensitivity, and noise sources of this channel are discussed.

I. Introduction

Since the early part of the Twentieth Century, physicists have relied on Einstein's Theory of General Relativity to explain many of the astrophysical phenomena that govern our universe. The theory documents in detail the effects of one of the fundamental forces of nature, gravity. General Relativity predicts that certain astrophysical events generate gravitational waves that propogate through spacetime, although no gravitational waves have ever been directly observed. The Laser Interferometer Gravitational Wave Observatory (LIGO) project attempts to observe such waves through the use of a network of Michelson Interferometers at various locations worldwide. Currently, LIGO has two sites: the LIGO Hanford Observatory (LHO) in Washington and the LIGO Livingston Observatory (LLO) in Louisiana. These interferometers will be used in conjunction with other collaborations worldwide to search for and confirm the detection of gravitational waves.

*Beneficiary of an NSF REU Grant. The author would like to thank the NSF and the entire staff of the LIGO Hanford Observatory for their assistance in this project.

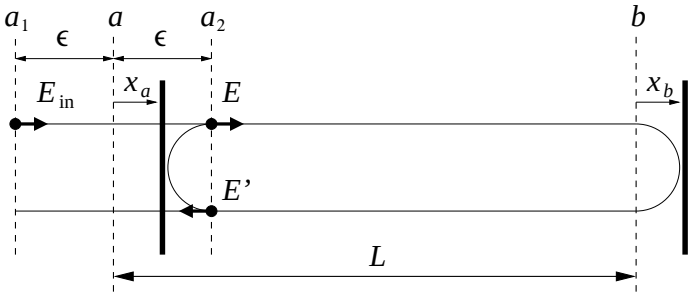

Figure 1: Optical setup of a dynamic Fabry-Perot Cavity [3]

The LHO interferometers are configured as power-recycled Michelson interferometers with Fabry-Perot cavity arms. Recent analysis of the properties of dynamic Fabry-Perot Cavities indicates that the sensitivity of the interferometer for non-optimal orientations to the strains characteristic of gravitational waves peaks at every free spectral range (FSR) of the incident light [1]. This study takes advantage of the increased sensitivity of the 4 km interferometer at its FSR of 37.5 kHz to develop a technique for gravitaional wave searches near this frequency. The technique utilizes a Stanford Research Systems SR830 lock-in amplifier to down-convert high frequency signals to the frequency range of a 2048 samples/sec LIGO data channel. The response of the interferometer, lock-in, and data channel are calibrated to obtain a working model. The sensitivity of the antisymmetric photodetector (ASPD) signal to interferometer length variations is determined experimentally and discussed.

II. Motivation

The motivation for this study comes from the paper *Dynamic resonance of light in Fabry-Perot cavities* by M. Rakhmanov, R.L. Savage Jr., D.H. Reitze, and D.B. Tanner[3]. The following summarizes the exposition of the fields and behavior of dynamic Fabry-Perot Cavities found in this work.

A Fabry-Perot Cavity is an optical setup that takes advantage of the resonance of light. As shown above, the cavity consists of two mobile mirrors set up a distance L apart. Laser light is sent to the cavity from the left side, with field $E_{in}(t)$. A small fraction of the incident light is transferred to the cavity, with the rest being reflected back. Light waves propogate back and forth through the cavity, transmitting a small fraction out at each end. For a cavity with fixed mirrors, when the laser wavelength is such that an integer multiple of the wavelength equals the round trip path length a resonance is reached and constructive interference occurs within the cavity.

For careful analysis of the interior field of a Fabry-Perot cavity, reference planes are defined. The mirror displacements from our reference points will be taken to be x_a and x_b for the front and back mirrors, respectively. A laser is directed to enter the cavity through the front mirror, transmitting some of its light to the cavity while having most reflected back at it. The transmissivities of the mirrors will be called t_a and t_b,

while their reflectivities will be known as r_a and r_b. The time required for a light beam to travel from one reference point to the other is given by

$$T = \frac{L}{c}, \tag{1}$$

where c is the speed of light. We use the standard angular frequency and wavenumber definitions for an electromagnetic wave:

$$\omega = 2\pi\nu \tag{2}$$

and

$$k = \frac{\omega}{c}, \tag{3}$$

where ν is the frequency of the light. Taking into account the finite propogation time of the wave, the distance seen by a ray of light moving through the cavity becomes:

$$d(t) = L + \delta L(t), \tag{4}$$

where

$$\delta L(t) = x_b(t-T) - x_a(t) \tag{5}$$

Resonance is achieved when $d(t)$ is an integer number of half wavelengths of the incident light. For a static cavity, resonance is observed periodically along the frequency range with period equal to the free spectral range of the light:

$$\nu_{fsr} = \frac{c}{2L} \tag{6}$$

or

$$\omega_{fsr} = \frac{\pi}{T} \tag{7}$$

Taking into account light propogation time and the boundary continuity of electromagnetic waves, the equation for the forward-propogating field in the cavity is found to be:

$$E(t) = t_a E_{in}(t) + r_a r_b e^{-2ik[L+\delta L(t)]} E(t-2T), \tag{8}$$

where $E_{in}(t)$ is the field of the incident light on the cavity, as shown in Figure 1.

The conditions for maintaining resonance in a Fabry-Perot cavity vary according to the variable parameters of the system. In a static cavity, the length and laser frequency will be constant and resonance will be achieved when

$$\frac{\delta\omega}{\omega} = -\frac{\delta L}{L}, \tag{9}$$

where $\delta\omega$ represents a variation in laser frequency and δL a variation in cavity length from resonance. In this case length and frequency variations are equivalent in

maintaining resonance. This is not true for dynamic cavities, where transition to the Laplace domain yields the resonance condition:

$$C(s)\frac{\delta\tilde{\omega}(s)}{\omega} = -\frac{\delta\tilde{L}(s)}{L}, \tag{10}$$

where s is complex and $C(s)$ is the normalized frequency-to-length transfer function

$$C(s) = \frac{1-e^{-2sT}}{2sT}. \tag{11}$$

To maintain resonance, changes in cavity length must be compensated for by variations in laser frequency. For small frequencies, $C(s)$ is approximately 1 and the condition for a static cavity is approached. As the input laser frequency increases, more and more frequency compensation is required for the same changes in cavity length. No frequency-to-length compensation is possible at FSR multiples, as C(s)=0 at these points.

A Pound-Drever Hall (PDH) negative-feedback locking signal is used to maintain resonance in the Fabry-Perot arms of the LIGO interferometers. This signal measures deviations from resonance and reports back to the laser, allowing it to adjust its frequency and continually lock the cavity to resonance. The PDH signal responds differently to length and laser frequency variations, producing two different transfer functions. For length variations, the transfer function $H_L(s)$ is given by:

$$H_L(s) = \frac{1-r_a r_b}{1-r_a r_b e^{-2sT}}. \tag{12}$$

As can be seen from Figures 2 and 3, $H_L(s)$ peaks at multiples of the cavity FSR. The response of the PDH signal to laser frequency variations is markedly different, with a transfer function $H_\omega(s)$ being given by:

$$H_\omega(s) = C(s)H_L(s) = \left(\frac{1-e^{-2sT}}{2sT}\right)\left(\frac{1-r_a r_b}{1-r_a r_b e^{-2sT}}\right). \tag{13}$$

As can be seen from Figure 4, $H_\omega(s)$ has zeros at frequency multiples of the cavity FSR. These zeros imply that the internal field of the cavity does not vary with frequency deviations at FSR multiples. At these frequencies the amplitude of the interior field remains steady while its phase changes with the phase of the laser.

The forms of the transfer functions $H_L(s)$ and $H_\omega(s)$ show that the cavity sensitivity to length changes is maximal at multiples of the FSR, while the sensitivity to laser frequency fluctuations is at a minimum. In the context of the LIGO interferometer, the length sensitivity peaks impliy that FSR multiples should be ideal for gravitational wave searches. However, since gravitational waves affect the cavity light as well as its length, an optimally oriented interferometer will show no response to gravitational waves for the optimal (directly overhead) orientation. Nonetheless, the interferometer sensitivity averaged over all orientations will still peak at FSR multiples. At the FSR, the gravitational wave sensitivity averaged over all sky positions and polarizations is about a factor of 5 worse than the length sensitivity [2]. The sensitivity peak is the basis for our study at 37.52 kHz, the FSR of the LHO 4 km interferometer (IFO).

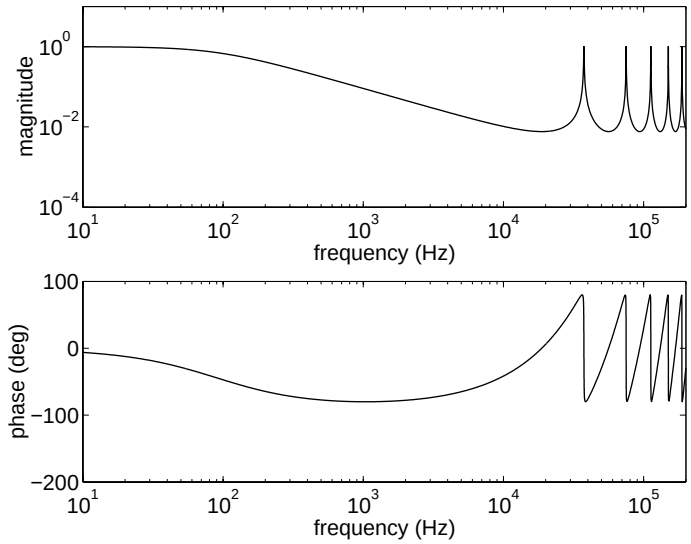

Figure 2: Bode Plot of the length-to-signal transfer function $H_L(s)$ [3].

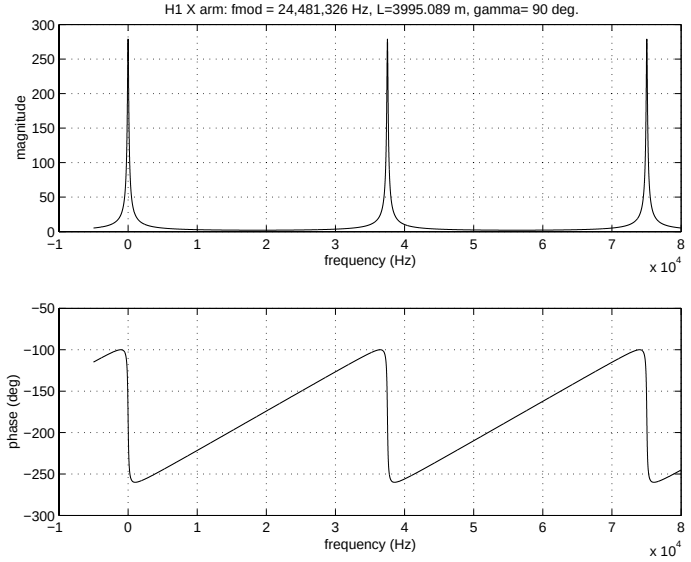

Figure 3: Linear plot of the magnitude and phase of the length-to-signal transfer function $H_L(s)$ emphasizing its periodic nature.

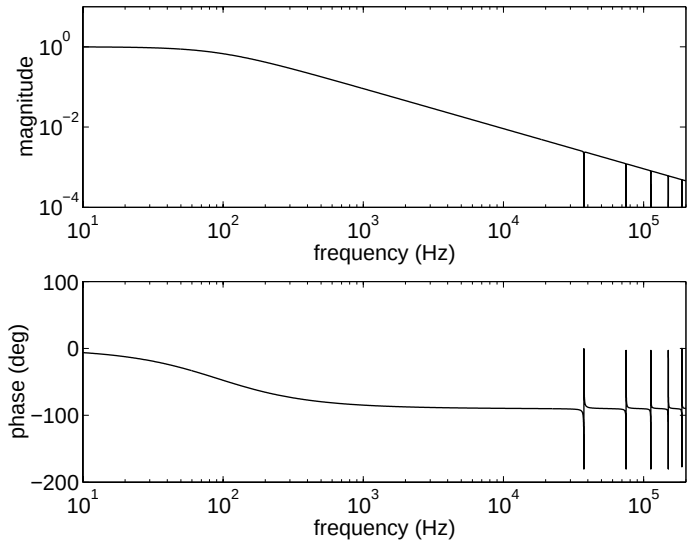

Figure 4: Bode Plot of the frequency-to-signal transfer function $H_{\omega}(s)$ [3].

III. Methods

To search for gravitational waves near 37.5 kHz, the following setup was implemented. As shown below, the output of the 4 km antisymmetric photodetector (ASPD) port AS2 was fed through a differential driver and sent to an SR830 lock-in amplifier. The lock-in amplifier allowed down-conversion of the signal by its reference frequency of 37 kHz and also provided amplification at its output. From there, the signal was sent through an anti-aliasing filter and into a DAQ ADCU (Data Acquisition Analog to Digital Converter Unit). The output of the ADCU was given to a 2048 Hz data channel and sent to the control room for analysis.

IV. Analysis

A. Hardware Analysis

To assess the performance of the down-conversion and readout scheme, calibration of both the hardware output of the channel and the ASPD response to cavity test mass displacement were performed. The first hardware element to be considered was the SR830 lock-in amplifier.

The lock-in was used here to down-convert data signals from high frequency to the sensitivity band of the selected LHO 2 kHz data channel. However, the traditional use of a lock-in is to determine the magnitude and phase of the input signal component at a predetermined reference frequency. From Fourier's Theorem, it is known that any signal can be represented as a sum of sine waves at varying frequencies and phases. The lock-in includes an internal oscillator to be set to the desired reference frequency.

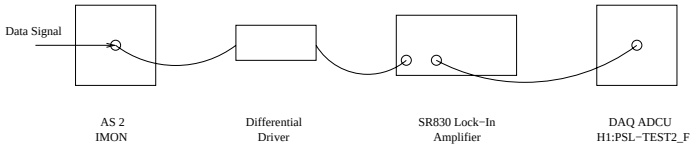

Figure 5: Setup of data acquisition and down-conversion hardware.

Input signals are fed into a mixer to be multiplied by the reference sine wave, producing outputs at different frequencies. The output of the first mixer is given by a sum of terms of the form:

$$\begin{aligned} V_{prod} = V_{sig}V_L sin(\omega_r t + \theta_{sig}) sin(\omega_L t + \theta_{ref}) = \\ \frac{1}{2}V_{sig}V_L cos([\omega_r - \omega_L]t + \theta_{sig} - \theta ref) - \\ \frac{1}{2}V_{sig}V_L cos([\omega_r + \omega_L]t + \theta_{sig} + \theta ref). \end{aligned} \tag{14}$$

Here $V_{sig}sin(\omega_r(t) + \theta_{sig})$ is the input signal and $V_L sin(\omega_L t + \theta_{ref})$ is the reference sinusoid. The mixer outputs signals at both the sum and difference of each input frequency with the reference frequency. We are generally interested in the difference terms, as this is the source of a DC signal from the component of the input signal at the referenece frequency. The mixer output is fed to a variable low pass filter, allowing the user to determine the rolloff of the output from the DC signal and eliminate the sum terms from the output. For an application where only a narrow neighborhood around the reference frequency component is desired, a long time constant may be set. Conversely, a short time constant is set for applications where a down-converted spectrum is required. The filtered signal is then passed to another mixer that multiplies it with the reference signal phase shifted by 90°. This allows the phase difference between the desired component and reference sine wave to be determined. An amplifier follows the second mixer to produce the final output.

In this study, the difference term in (14) is exploited for the purpose of down-converting signals at the 4 km IFO FSR frequency. The time constant of the low pass filter is set to its minimal setting of 10 μs to prevent filtering of the data in our small bandwidth. The range of data examined through the 2048 Hz LHO data channel was from 0 to 900 Hz, leaving only some difference terms of the first mixer output. Since cosine is even, difference terms with frequencies on either side of the reference are observed equally, causing them to overlap in the output. With the lock-in set to 37 kHz, overlapping data bands from 0 to 900 Hz on both sides of 37 KHz were observed (37 kHz to 36.1 kHz and 37 kHz to 37.9 kHz). Only the higher band was desired here. The effect of the overlap of the lower band was lessened by the much greater length sensitvity in the FSR band. To more completely remove the overlap signal, a high pass filter for the reference frequency could be put onto the input of the lock-in.

B. Amplitude Calibration

To determine the amplitude response of the setup, the gain on the lock-in output and the characteristics of the Analog to Digital Converter (ADC) were examined. Several "sanity check" trials were performed, with one representative trial described below.

A Stanford DS340 function generator was set to provide a 37.5 kHz sine wave at 0.10 V_{pp} and then connected to the SR830 lock-in amplifier. The reference frequency of the lock-in was set to 37 kHz, resulting in an output that down-converted the DS340 signal frequency to 500 Hz. The amplitude of the lock-in output at 500 Hz was given by:

$$V_{out} = \left(\frac{R(\mathrm{V_{rms}})}{\mathrm{Sensitivity}(\mathrm{V_{rms}})} - \mathrm{Offset} \right) \times \mathrm{Expand} \times 10\mathrm{V}, \tag{15}$$

where R was the amplitude of the input signal at 500 Hz. Here the sensitivity, offset, and expand of the lock-in were set to 500m$\mathrm{V_{rms}}$, 0, and 1 respectively. Thus the output was a 500 Hz sine wave with amplitude 1.41 V_{pp} or 0.5 V_{rms} as verified by a Tektronix TDS3034B oscilloscope. This waveform was subsequently sent to the ADC, where the data was converted into 16 bit digital format. The Diagnostic Test Tools (DTT) program used a Fast Fourier Transform (FFT) algorithm to produce a power spectrum in Power Spectral Density (PSD) units. The peak of this plot was converted to V_{rms} as follows:

$$V_{rms} = \frac{4N\sqrt{\mathrm{BW}}}{2^{16}}(\mathrm{volts}), \tag{16}$$

where N represents the magnitude in count number of the peak and BW is the selected bandwidth of the FFT tool. The expected value for V_{rms} based on the input to the ADC was 0.5V, and this was very nearly matched by the program output for several trials. The time series of the output data was also checked, and this revealed the expected 8192 counts per volt of input as well as an offset of approximately -200 counts.

C. Length Calibration

A drive of the X arm Input Test Mass (ITMX) was performed to determine the ratio between test mass displacement and ASPD voltage output. This required the 4k interferometer to be locked in common mode, and the calibration was done with the setup shown in Figure 6. Note that the laser was at 0.8 W low power. As pictured below, a Stanford Research Systems SR785 Dynamic Signal Analyzer was set to source a 1.0 $\mathrm{V_{pp}}$ sine wave. The output was split and sent to two SR560 pre-amplifiers with a gain of 5 each and then into the drive ports of the ITMX. The Lower Right (LR) and Upper Left (UL) coils of the test mass were given non-inverted signals while the Upper Right (UR) and Lower Left (LL) coils were given inverted drive signals. This forced a pendulum-like oscillation of the ITMX test mass whose amplitude was captured by the ASPD and read back to the SR785. The SR785 swept sine measurement was used to generate a transfer function between the ASPD signal and the original source out. Plots of this transfer function for two different frequency spans are shown in Figures

7 and 8. The expected peak in response to length variation is observed at the 4k FSR of 37.52 kHz. The origin of the additional narrow spiking feature above the FSR is currently unknown.

The drive transfer function was used to calibrate the test mass displacement reflected in the output voltage signal of the ASPD. The test mass was known to respond to the drive as a simple pendulum, with a transfer function proportional to $(f_o/f)^2$, where f_o was known to be 0.761 Hz. This feature allowed extrapolation of the DC calibration done by Michael Landry to the frequency neighborhood of the 4k FSR. First the drive at the suspension controller was calibrated by converting from digital to analog, applying the pendulum $(f_o/f)^2$ relation to the DC calibration, and taking into account the relevant filtering. In this case there was a pole at 4 Hz and a zero at 30 Hz in the suspension controller, resulting in a reduction factor of 7.5 above about 50 Hz. We note also that the test mass displacement represents twice the motion see when the whole interferometer is used to sense the differential motion. The relation between test mass displacement and suspension control was found to be:

$$[M]\left[\frac{16384\text{counts}}{1V_{\text{coil(DC)}}}\right]\left[\left(\frac{f_o}{f}\right)^2\left(\frac{V_{\text{coil(DC)}}}{V_{\text{coil(AC)}}}\right)\right]\left[\frac{1}{7.5}\frac{V_{\text{coil(AC)}}}{V_{\text{drive}}}\right] = 1.6\times10^{-16}\frac{\text{m}_{\text{ITMX}}}{V_{\text{drive}}}, \quad (17)$$

where

$$\begin{aligned} M &= 0.17992\text{nm/count} \\ f_o &= 0.761\text{Hz} \end{aligned} \quad (18)$$

were the DC calibration factor and characteristic frequency, respectively. The corresponding differential motion ratio was 8.1 $\times10^{-17}$ m_{diff} / V_{drive}. We now use the transfer function to quantify the response of the ASPD to the SR785 input:

$$\left[T\left(\frac{V_{ASQ}}{V_{785}}\right)\right]\left[\frac{1}{A}\left(\frac{V_{785}}{V_{560}}\right)\right] = 2.8\times10^{-5}\frac{V_{ASQ}}{V_{560}} \quad (19)$$

where T was the transfer function response near 37.52 kHz and A was the amplification factor of the SR560 pre-amps. Their values were:

$$\begin{aligned} T &= -77\text{dB} \\ A &= 5. \end{aligned}$$

Here, our drive signal sent to the suspension controller was the output of the SR560 pre-amplifiers. When we substitute this in for V_{drive} we may divide our first result by our second result to obtain the final signal to displacement ratio:

$$\frac{\left[1.6\times10^{-16}\frac{\text{m}_{\text{ITMX}}}{V_{560}}\right]}{\left[2.8\times10^{-5}\frac{V_{ASQ}}{V_{560}}\right]} = 5.7\times10^{-12}\frac{\text{m}_{\text{ITMX}}}{\text{V}_{\text{ASQ}}} \quad (20)$$

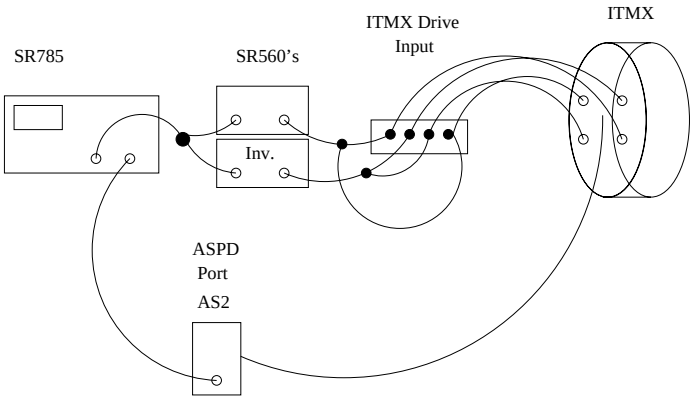

Figure 6: Hardware Setup for ITMX length calibration drive.

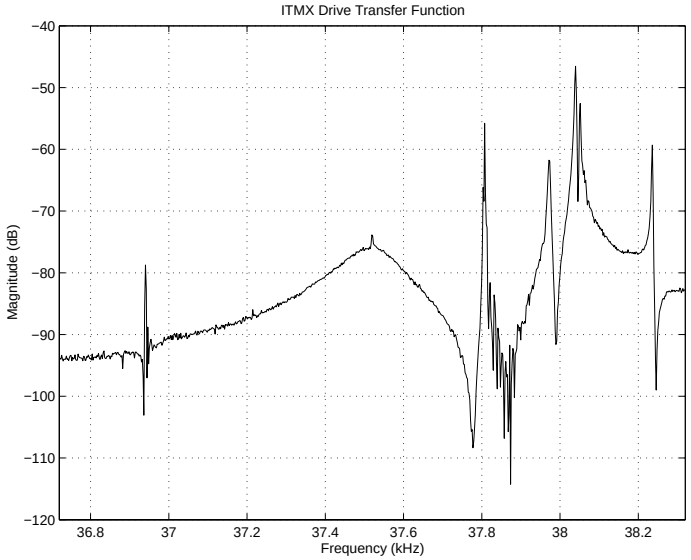

Figure 7: ASPD QMON transfer function response for ITMX drive, 1600 Hz span.

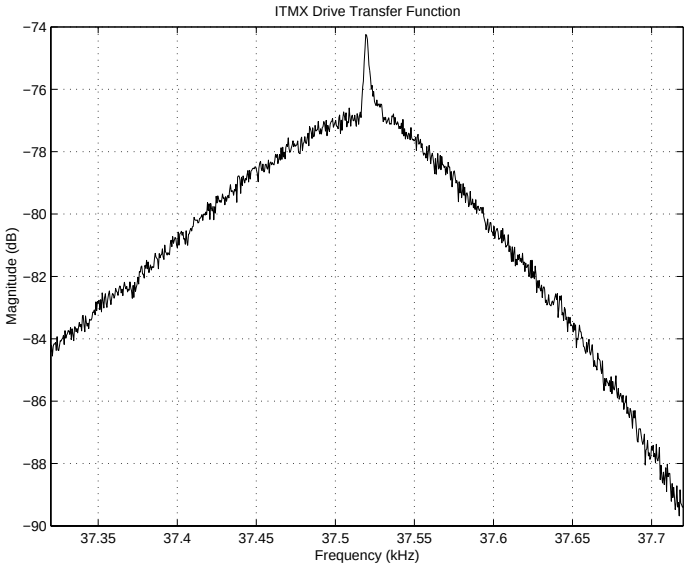

Figure 8: ASPD QMON transfer function response for ITMX drive, 400 Hz span.

The corresponding differential conversion factor is 2.9 $\times 10^{-12}$ m_{diff} / V_{ASQ}. Using the test mass displacement conversion we note that the ITMX drive generated a peak-to-peak displacement of 8.1 $\times 10^{-16}$m.

D. Length Sensitivity Determination

With the conversion between ASPD voltage signal and test mass displacement in hand, a determination of the channel sensitivity to length variations was possible. To that end, a power spectrum of the ASPD QMON signal was taken, again with the interferometer in low power common mode lock. This power spectrum provided the noise level of the channel and was seen to dip near the FSR, as shown in Figure 9.

The dip may be indicative of frequency dependent noise characteristic of the zero in the frequency-to-signal transfer function $H_\omega(s)$ at FSR multiples. To find the length sensitivity of the channel, the QMON noise spectrum was divided by the ITMX drive transfer function in length units. As can be seen in Figures 10 and 11, the sensitivity of the channel to length variations is best at the cavity FSR, reaching down to approximately 5 $\times 10^{-19}$ m / $\sqrt{\text{Hz}}$. For a broader frequency band the length sensitivity is about 2 $\times 10^{-18}$ m / $\sqrt{\text{Hz}}$, which would correspond to a gravitational wave sensitivity of about 1 $\times 10^{-17}$ m / $\sqrt{\text{Hz}}$ (averaged over all polarizations and orientations as discussed above).

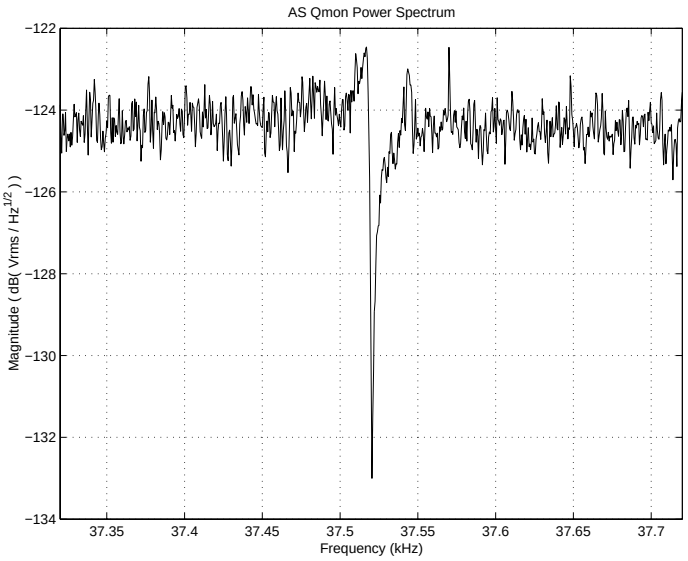

Figure 9: Power Spectrum of noise level of ASPD QMON with IFO in low power common mode lock, 400 Hz span.

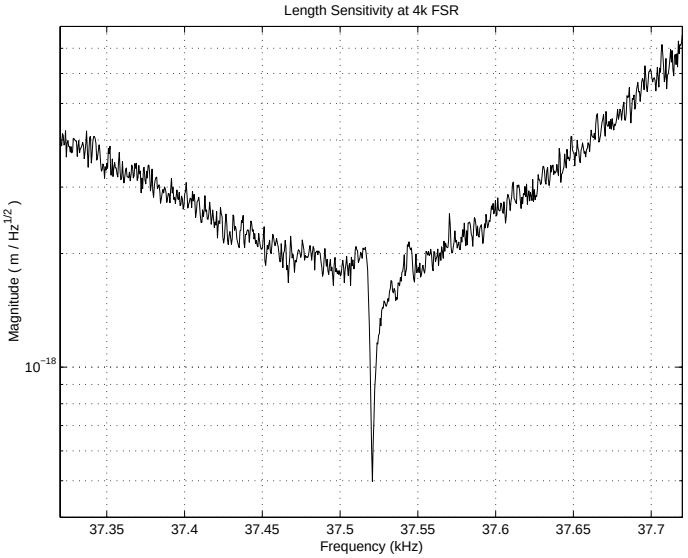

Figure 10: Length Sensitivity of 4k IFO with 400 Hz span centered at 37.52 kHz.

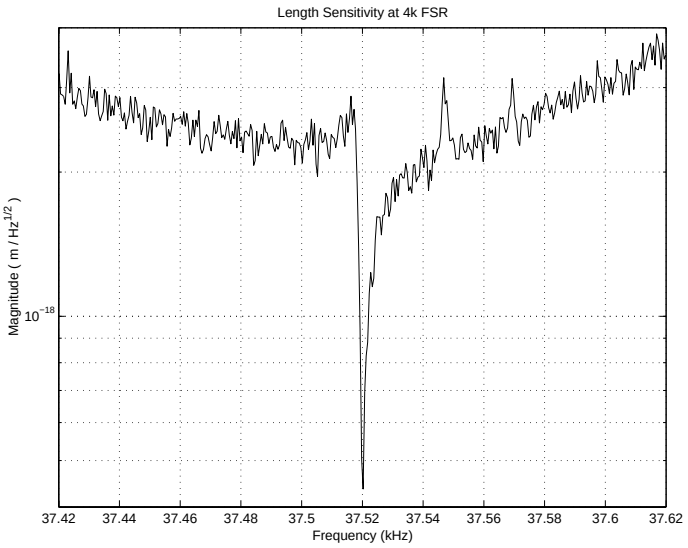

Figure 11: Length Sensitivity of 4k IFO with 200 Hz span centered at 37.52 kHz.

E. Noise Distribution

With the calibration in place, a brief sample of channel data was taken. Data was collected for 2 minutes at the 2048 Hz sampling rate of the channel and histogrammed as shown in Figure 9. As expected the distribution was approximately Gaussian, indicating white noise. To understand the channel output on a more rigorous level, a noise spectrum must be analyzed in the frequency domain and its sources determined. In this case, the primary noise source appeared to be 60 cycle electronics noise, but further study is required. Categorizing the noise sources would allow one to differentiate between a possible gravitational wave signal and other sources of spikes in a power spectrum or glitches in a time series. One possible gravitational wave source around 37.5 kHz could be neutron star modes. However, the expected energy radiated in these high frequency modes is expected to be small so the signals are likely to be very weak (Private communication with G. Mendell).

V. Conclusions

During this project, a method for down-converting interferometer signals at the 4 km IFO FSR of 37.52 kHz was implemented and tested. The SR830 lock-in amplifier was installed and used for down-conversion of gravitational wave channel signals to the data range of the 2 kHz channel H1:PSL-TEST2_F. The lock-in was determined to be adequate for frequency down-conversion, with its output characterized in terms of its frequency window and amplification. The sensitivity of the 4k IFO to ITMX length displacement near 37.5 kHz was found to be approximately 2×10^{-18} m / $\sqrt{\text{Hz}}$, with a dip down to 5×10^{-19} m / $\sqrt{\text{Hz}}$ at the FSR frequency. However, the sensitivity

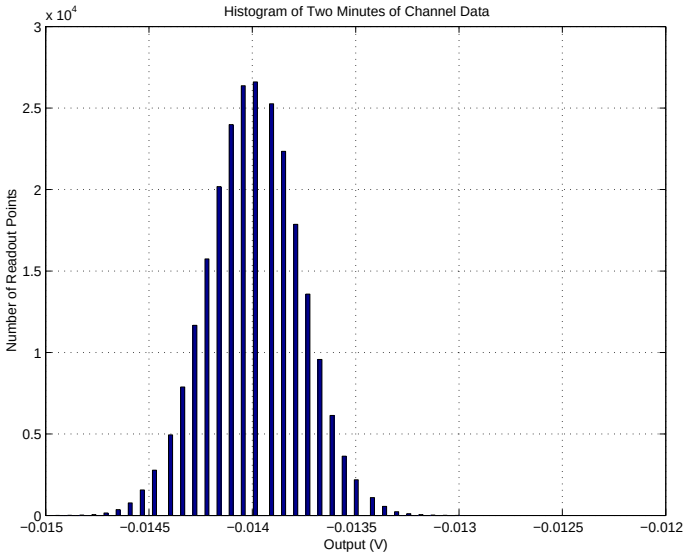

Figure 12: Histogram of two minutes of channel data with lock-in setup.

to gravitational wave strains averaged over all orientations has been proposed to be approximately 5 times worse [2]. A sample of actual channel data was plotted into a histogram to reveal a noise signal that was approximately Gaussian, indicating white noise. Further studies of the possible gravitational wave sources and noise sources at the 4k FSR frequency of 37.5 kHz must be conducted to utilize the length sensitvity peak of the LHO 4 km interferometer observed at this frequency.

References

[1] Schilling, R.: *Class. Quantum Grav.*, 14 (1997) 1513-1519

[2] Daniel Sigg: *Strain Calibration in LIGO*, Technical Note LIGO-T970101-B-D (2003)

[3] M. Rakhmanov, R.L. Savage Jr., D.H. Reitze, and D.B. Tanner: *Dynamic resonance of light in Fabry-Perot cavities*, Physics Letters A 305, p. 239-244 (2002)